



1 **Hydrologic modeling of a Himalayan mountain basin by using the SWAT model**

2
3
4
5
6
7

Sharad K. Jain^{1*}, Sanjay K. Jain¹, Neha Jain¹ and Chong-Yu Xu²

¹National Institute of Hydrology, Roorkee 247667, India

² University of Oslo, Oslo, Norway

*Corresponding Author: Email s_k_jain@yahoo.com

8 **ABSTRACT**

9 A large population depends on runoff from Himalayan rivers which have high hydropower
10 potential; floods in these rivers are also frequent. Current understanding of hydrologic response
11 mechanism of these rivers and impact of climate change is inadequate due to limited studies. This
12 paper presents results of modeling to understand the hydrologic response and compute the water
13 balance components of a Himalayan river basin in India viz. Ganga up to Devprayag. Soil and
14 Water Assessment Tool (SWAT) model was applied for simulation of the snow/rainfed catchment.
15 SWAT was calibrated with daily streamflow data for 1992-98 and validated with data for 1999-
16 2005. Manual calibration was carried out to determine model parameters and quantify uncertainty.
17 Results indicate good simulation of streamflow; main contribution to water yield is from lateral and
18 ground water flow. Water yield and ET for the catchments varies between 43-46 % and 57-58% of
19 precipitation, respectively. The contribution of snowmelt to lateral runoff for Ganga River ranged
20 between 13-20%. More attention is needed to strengthen spatial and temporal hydrometeorological
21 database for the study basins for improved modeling.

22 Keywords: Hydrological modeling, SWAT, Western Himalaya, calibration

23
24

1 INTRODUCTION

25 Many rivers, springs and lakes in the mountain regions are fed by significant contribution runoff
26 from snow and glacier melt. The headwater catchments of most of the rivers in the Himalayan
27 region such as the Ganga, the Indus and the Brahmaputra, lie in the snow covered areas. Snowfall
28 is temporarily stored in high hills and the melt water reaches the river later in the hot season. Snow
29 and glacier runoff are vital in making big Himalayan Rivers perennial whereas the rainfall
30 contribution during the monsoon season is important for high flow volumes in rivers. Snow
31 accumulates in the Himalayas generally from November to March, while melt season spans the
32 months April to September. Snowmelt is the predominant component of runoff in mountains in
33 April to June months and it forms a significant constituent of streamflows during July - September.

34 High spatial and temporal variability in hydro-meteorological conditions in mountainous
35 environments requires spatial models that are physically realistic and computationally efficient
36 (Liston and Elder, 2006b). Among the models developed to simulate hydrological response of
37 mountainous basins, the most common approach followed for distributed snowmelt modeling in the
38 absence of detailed measured data is to subdivide the basin into zones based upon elevation,
39 allowing the model to discretize the snowmelt process based on watershed topography (Hartman et



40 al., 1999; Li et al., 2013, 2015, 2016). The list of models developed for modeling response of a
41 catchment subject to solid and liquid precipitation includes commercial software such as Mike-SHE
42 (<http://mikebydhi.com>) and the public domain models such as the SWAT model (Neitsch, 2002), the
43 Xinanjiang Model (Zhao et al., 1995) and the HBV model (Bergstrom, 1992). An obvious advantage
44 of the public-domain models is the saving in cost and ease in sharing model set-ups. SWAT is a
45 public-domain model that has been used extensively. A user-friendly interface to set-up the model
46 in a GIS framework, detailed user's manual and a large user base are the main reasons for a number
47 of applications of the SWAT model.

48 SWAT is a semi-distributed, continuous watershed modelling system, which simulates
49 different hydrologic responses using process based equations. Most of the applications of the
50 SWAT model have used daily or monthly time steps for simulation. Obviously, it has been
51 comparatively easy to obtain higher values of Nash-Sutcliffe Efficiency (NSE) for monthly data
52 than for the daily data. Further, SWAT model has been successfully applied to catchments with size
53 of a few sq. km to thousands of sq. km. For example, Spruill et al., 2000 applied the SWAT model
54 to simulate daily streamflows in a watershed in Kentucky covering an area of 5.5 km² whereas
55 Zhang et al., 2008 used it to simulate monthly runoff of a mountainous river basin in China
56 covering area of 114,345 km². Some more recent applications of SWAT for rainfall-runoff
57 modeling are those by Jain et al., 2010, Shawul et al., 2013, Kushwaha and Jain, 2013, Khan et al.,
58 2014, Tamm et al., 2016, Awan et al., 2016 and Singh et al., 2016. Tyagi et al., 2014 used it for
59 sediment modelling and Pandey et al., 2014 and Tamm et al., 2016 used results of SWAT to
60 estimate hydropower potential of a catchment.

61 Many studies have attempted to simulate water quality variables by employing the SWAT
62 model. Jha et al., 2006 simulated streamflow, sediment losses, and nutrient loadings in the Raccoon
63 River watershed and assessed impacts of land use and management practice shifts. Hafiz et al.,
64 2012 examined applied the SWAT model to model flow, sediments and water quality parameters in
65 upper Thachin River Basin, Thailand with catchment area of 5,693 km². It was reported that the
66 model gave good results. Qiu and Wang, 2014 applied the SWAT model to the Neshanic River
67 watershed to simulate streamflow and water quality parameters including total suspended solids
68 (TSS), total nitrogen (TN), and total phosphorus (TP). An attractive feature of the SWAT model is
69 its ability to model the catchment response due to snow/glacier melt and rainfall. Many studies have
70 harnessed this feature of the model. For instance, Lemonds et al., 2007 calibrated the SWAT model
71 to the Blue River basin (867 km²) in Colorado (USA) by adjusting the snowmelt, snow formation,
72 and groundwater parameters and obtained good fits to average monthly discharge values (NSE =
73 0.71). As per Stehr et al., 2009, the snow component of SWAT was capable of providing a
74 reasonably good description of the snow-cover extension over a small Chilean Basin (455 km²).
75 Pradhanang et al., 2011 compared snow survey data for the catchment of Cannonsville reservoir
76 with model simulated snowpack and snowmelt at different elevation bands. When measured and
77 simulated snowpack were compared, correlation coefficients ranging from 0.35 to 0.85 were
78 obtained. Simulations of daily and seasonal streamflow improved when 3 elevation bands were
79 used. Troin and Caya, 2014 demonstrated the ability of SWAT to simulate snowmelt dominated



80 streamflow in the Outardes Basin, Quebec (Canada). The calibration of SWAT model showed a
81 satisfactory performance at the daily and seasonal time scales.

82 To improve the snow/glacier melt section of SWAT, some authors have attempted to
83 develop and plug-in routines for these processes. For example, Fontaine et al., 2002 developed a
84 snowfall-melt routine for mountainous terrain for the SWAT model which improved the correlation
85 between observed and simulated stream flow. Recently, Luo et al., 2013 proposed a dynamic
86 Hydrological Response Unit approach and incorporated an algorithm of glacier melt,
87 sublimation/evaporation, accumulation, mass balance and retreat into the SWAT model. They
88 simulated the transient glacier retreat and its impacts on streamflow at basin scale. This updated
89 model was applied in the Manas River Basin (MRB) in northwest China and the authors obtained
90 NSE of 0.65 for daily streamflow and small percent bias of 3.7% in water balance. The
91 hydrological community at large can make good use of such innovations if the relevant software
92 and guidelines for data preparation are made easily available.

93 Many other models or frameworks have been used in the recent past for modelling mountain
94 catchments. Shrestha et al. (2013) developed energy budget-based distributed modeling of snow
95 and glacier melt runoff in a multilayer scheme for different types of glaciers within a distributed
96 biosphere hydrological modeling framework. A study of Hunza River Basin (13,733 km²) in the
97 Karakoram mountains where the SWAT model was used showed good agreement with observations
98 (NSE = 0.93). Likewise, Immerzeel et al. (2013) used results from an ensemble of climate models
99 along with a glacio-hydrological model for assessment of the impact of climate change on
100 hydrologic response of two Himalayan watersheds: the Baltoro (Indus) and Langtang (Ganges).
101 Future runoff was found to increase in both watersheds. A large uncertainty in future runoff arising
102 from variations in projected precipitation between climate models was noted. It is hoped that the
103 numerous attempts to apply the existing models to different geographies and research to develop
104 new modeling theories would lead to significant advances in hydrology of mountain basins across
105 the world.

106 Hydrological modeling of Himalayan river basins is important for many reasons. Nearly 2
107 billion people depend upon the waters of these rivers. Since most of these rivers are perennial and
108 the terrain has steep slopes, they have huge hydropower potential whose exploitation requires a
109 sound understanding of hydrologic response mechanism. Further, water triggered disasters are also
110 frequent in these basins. The region has complex topography and hydrologic data are scarce. In
111 addition, changes in land use/cover and climate are likely to significantly impact snow/glacier
112 accumulation and melt and hydrological response of these river basins. Snow and glacier melt
113 significantly contribute to flow of most Himalayan rivers and their modeling is an important
114 component in streamflow modeling of Himalayan rivers. Global warming is likely to accelerate
115 snow and glacier melt and it is necessary to study its impact for long term water resources planning.
116 However, in spite of well-recognized importance and need of such studies, not many attempts have
117 been made to assess hydrology of these rivers.



118 Clearly, there is a need for better understanding of the hydrologic response of the
119 Himalayan rivers for sustainable water management, developing the ability to forecast floods, and
120 predict the impacts due to changes in climate and land use/cover. To that end, a distributed model is
121 needed whose data requirements match with the availability. Although studies have been carried out
122 in mountainous catchments with a variety of topography, climate, and data availability by using the
123 SWAT model and the results have been quite good, only limited studies have been carried out in the
124 Indian Himalayan region. The hydrological and other data of this region that are needed for
125 modeling are not easily available and considerable efforts are required to collect and process the
126 data and setup a distributed model. Therefore, the objective of this study was to improve our
127 understanding of hydrological regime of the Himalayan rivers and enhance prediction of a
128 hydrological processes. The main goal was achieved through carrying out hydrologic modeling of a
129 Himalayan river basin which receives contribution from snow/glacier and rainfall by employing
130 larger amount of observed data. We have also attempted to determine various water balance
131 components for better understanding of hydrologic response of the watershed. Better modeling and
132 hydrologic assessment of these basins will help in improved management of water resources,
133 harness hydropower potential, and partly overcome problems due to data scarcity. Such studies will
134 also help understand the likely impacts of climate change on water resources.

135 Before proceeding further the SWAT model is briefly described in the following.

136 **2 THE SWAT MODEL**

137 The Soil and Water Assessment Tool (SWAT) is a semi-distributed, continuous time watershed
138 modelling system which simulates hydrologic response of a catchment by using process-based
139 equations. It has been developed by the USDA Agricultural Research Service (Arnold et al., 1998).
140 Spatial variability in a catchment are represented in SWAT by dividing the catchment area into sub-
141 watersheds; these are further subdivided into hydrologic response units (HRUs). A HRU possesses
142 unique land use, soil types, slope and management practices (Neitsch et al., 2002a, 2002b). To
143 compute the water balance, the model simulates a range of hydrologic processes such as
144 evapotranspiration, snow accumulation, snowmelt, infiltration and generation of surface and
145 subsurface flow components.

146 SWAT model allows division of maximum ten elevation zones in each sub-basin to consider
147 orographic effects on precipitation, temperature and solar radiation (Neitsch et al., 2001). Snow
148 accumulation, sublimation and melt are computed in each elevation zone and weighted average is
149 computed subbasin wise. Snowmelt depth in the same elevation band is assumed to be the same in
150 all sub-basins.

151

152 **2.1 Modeling of Snowmelt**

153 A temperature-index approach is used by SWAT model to estimate snow accumulation and
154 melt. Snowmelt is calculated as a linear function of the difference between the average snowpack
155 maximum temperature and threshold temperature for snowmelt. Snowmelt is combined with
156 rainfall while calculating infiltration and runoff. SWAT does not include an explicit module to
157 handle snow melt processes in the frozen soil, but includes a provision for adjusting infiltration and



158 estimating runoff when the soil is frozen (Neitsch et al., 2005). Despite this limitation, SWAT is
 159 considered to be an appropriate integrated model for addressing a range of issues. It is noted that
 160 many of the existing models do not have the capability to model both snow/glacier melt and
 161 rainfall-runoff processes.

162 In the temperature-index approach, temperature is a major factor that controls snowmelt
 163 (Hock, 2003). Snowmelt is computed as a linear function of the difference between average
 164 snowpack maximum temperature and the threshold temperature for snowmelt, SMTMP:

$$165 \quad SNO_{mli} = b_{mli} \cdot SNO_{covi} \left[\frac{T_{snowi} + T_{maxi} - SMTMP}{2} \right] \quad (1)$$

166 Where SNO_{mli} is the amount of snowmelt on day i (mm H₂O), T_{maxi} is the maximum air
 167 temperature on day i (°C), SMTMP (°C) is snowmelt base temperature above which snow will be
 168 allowed to melt and b_{mli} is the melt factor on day i (mm H₂O-day). Snowmelt is included with
 169 rainfall in computation of infiltration and runoff.

170 The classification of precipitation is based on a threshold value of mean air temperature. If
 171 the average daily air temperature is below the snowfall temperature, the precipitation in a HRU is
 172 considered as solid (or snow) and the liquid water equivalent of the snowfall is added to snowpack.
 173 The snowpack is depleted by snowmelt or sublimation. The mass balance for the snowpack for a
 174 HRU is:

$$175 \quad SNO_i = SNO_{i-1} + P_s - E_{subi} - SNO_{mli} \quad (2)$$

176 where, SNO_i is the water content of the snowpack (mm H₂O), P_s is the water equivalent of snow
 177 precipitation (mm H₂O), E_{subi} is the amount of snow sublimation (mm H₂O), and SNO_{mli} is the
 178 water equivalent of snow melt (mm H₂O), all for day i .

179 The spatial non-uniformity of the areal snow coverage over the HRU is taken account
 180 through an areal snow depletion curve that describes the seasonal growth and recession of the
 181 snowpack (Anderson, 1976). Two addition parameters are defined at the watershed scale,
 182 SNOCOVMX and SNO50COV. These control the areal depletion curve by accounting for the
 183 variable snow coverage as:

$$184 \quad SNO_{covi} = \frac{SNO_i}{SNOCOVMX} \left[\frac{SNO_i}{SNOCOVMX} + \exp\left(cov_1 - cov_2 \cdot \frac{SNO_i}{SNOCOVMX} \right) \right]^{-1} \quad (3)$$

185 where SNO_{covi} is the fraction of HRU area covered by snow on the day i , SNO_i is the water content
 186 of the snow pack on day i , SNOCOVMX is the minimum snow water content that correspond to
 187 100% snow cover (mm H₂O), and cov_1 and cov_2 are coefficients that control the shape of the curve.

188 2.2 Modeling of Catchment Hydrology

189 Weather, soil properties, topography, vegetation and land management practices are the most
 190 important inputs for the SWAT model. SWAT computes actual soil water evaporation using an
 191 exponential function of soil depth and water content. The modified Soil Conservation Service



192 (SCS) curve number method is used to compute runoff. The influence of plant canopy infiltration
193 and snow cover is incorporated into the runoff calculation. To support soil water processes such as
194 infiltration, evaporation, plant uptake, lateral flow, and percolation to lower layers, the soil profile
195 is subdivided into many layers. When field capacity of a soil layer is exceeded downward flow
196 occurs and the layer below is not saturated. Percolation from the bottom of the soil profile recharges
197 the shallow aquifer. Lateral sub-surface flow in the soil profile is calculated simultaneously with
198 percolation. Groundwater flow contribution to total stream flow is simulated by routing the shallow
199 aquifer storage component to the stream. Runoff is routed through the channel network by the
200 variable storage routing method or the Muskingum method (Neitsch et al., 2005).

201 SWAT model simulates hydrologic cycle based on the water balance equation:

$$202 \quad SW_t = SW_o + \sum_{i=1}^n (R_{day} - Q_{surf} - E_a - w_{seep} - Q_{gw}) \quad (4)$$

203 where, SW_t is the final soil water content (mm H₂O), SW_o is the initial soil water content (mm
204 H₂O), t is time in days, R_{day} is amount of precipitation on day i (mm H₂O), E_a is the amount of
205 evapotranspiration on day i (mm H₂O), Q_{surf} is the amount of surface runoff on day i (mm H₂O),
206 w_{seep} is the amount of percolation and bypass exiting the soil profile bottom on day i (mm H₂O),
207 and Q_{gw} is the amount of return flow on day i (mm H₂O).

208 Since the model maintains a continuous water balance, the subdivision of the watershed in
209 HRUs enables the model to consider differences in evapotranspiration for different crops and soils.
210 Runoff is predicted separately for each sub area and is routed to compute total runoff for the basin.

211 SWAT model software and documentation are freely available through Internet at
212 <http://swat.tamu.edu/software/swat-executables/>.

213

214 **2.3 Temperature index with elevation band approach**

215 This method incorporates elevation and temperature which is used to determine the snow
216 pack and snowmelt caused by orographic variation in precipitation and temperature. Many studies,
217 e.g., Zhang et al. (2008), have shown that elevation is an important factor in the variation of
218 temperature and precipitation. Fontaine et al. (2002) introduced a modified snowfall-snowmelt
219 routine for mountainous terrain into SWAT. This modified routine allows the SWAT model to
220 divide each sub-basin into 10 elevation bands and simulates the spatial and temporal variation of
221 snowpack and snowmelt on account of elevation. The temperature and precipitation for each
222 elevation band was adjusted by using:

223

$$224 \quad T_B = T + (Z_B - Z) \cdot dT / dZ \quad (5)$$

$$225 \quad P_B = P + (Z_B - Z) \cdot dP / dZ \quad (6)$$



226 Where, T_B is the mean temperature ($^{\circ}\text{C}$) in the elevation band, T is the temperature measured at the
227 weather station ($^{\circ}\text{C}$), Z_B is the midpoint elevation of the band (m), Z is the elevation (m) of the
228 weather station, P is the precipitation measured at the weather station (mm), P_B is the mean
229 precipitation of the band (mm), dP/dZ is the precipitation lapse rate (mm/km), and dT/dZ is the
230 temperature lapse rate ($^{\circ}\text{C}/\text{km}$).

231

232 3 THE STUDY AREA AND DATA USED

233 In the present study, Ganga River Basin up to Devprayag have been considered. The study area lies
234 in the North- Western Himalayan ranges, between latitudes 30° to $31^{\circ} 30'$ North and longitudes 78°
235 $7'$ to $80^{\circ} 15'$ East in India and is shown in Figure 1. The size of the catchment is about 18728
236 km^2 and elevation varies from 427 m to 7785 m. Bhagirathi and Alaknanda Rivers are the two
237 headwater streams that join at Devprayag to form Ganga River. The Bhagirathi River originates
238 from the snout of the Gangotri Glacier at Gomukh (3900 m). It flows for 217 km to reach
239 Devprayag and is joined by Bhilangana and Asiganga Rivers on the way. Asiganga joins Bhagirathi
240 River at 5 km upstream (1120 m) of Uttarkashi from west direction. Bhilangana River originates
241 from Khatling glacier (3950 m) and joins the Bhagirathi River at Tehri from east direction.
242 Alaknanda River rises at the confluence and the foot of the Satopanth and Bhagirath Kharak
243 Glaciers. The Alaknanda River flows for about 224 km before meeting with Bhagirathi River at
244 Devprayag. Its main tributaries are Dhaulti Ganga, Pindar, Nandakini and Mandakini. The average
245 rainfall in the study area varies between 1000 to 2500 mm, of which 60-80% falls during the
246 monsoon period between June and September. The rivers experiences strong seasonal climatic
247 variations, which is also reflected in the monthly variation in stream flows. High flow takes place
248 during June-September, when the combined influence of rainfall and snow melt is at the maximum.

249 In this study, a number of maps have been prepared. The sources and resolution of ASTER
250 DEM, land use land cover map and soil map are given in Table 1.

251 Meteorological data for the study area consisted of 16 years of time series (1990-2005) of
252 daily precipitation, minimum and maximum temperature, solar radiation and wind speed for 7
253 stations, namely Badrinath, Joshimath, Karanprayag, Rudraprayag, Uttarkashi, Tehri and
254 Devprayag. The rainfall data obtained for these stations were having many gaps. Therefore,
255 precipitation data from *Asian Precipitation - Highly-Resolved Observational Data Integration*
256 *Towards Evaluation of Water Resources* (APHRODITE's Water Resources) were used. The
257 APHRODITE project develops state-of-the-art daily precipitation datasets with high-resolution
258 grids for Asia. The datasets are created primarily with data obtained from a rain-gauge-observation
259 network. APHRODITE's Water Resources project has been conducted by the Research Institute for
260 Humanity and Nature (RIHN) and the Meteorological Research Institute of Japan Meteorological
261 Agency (MRI/JMA) since 2006. A daily gridded precipitation dataset for 1961-2007 was created by
262 collecting rain gauge observation data across Asia through the activities of the APHRODITE
263 project (<http://www.chikyu.ac.jp/precip/>). The final data product does not have any gaps.

264 APHRODITE data is available in the form of grid of $0.5^{\circ}\times 0.5^{\circ}$ and $0.25^{\circ}\times 0.25^{\circ}$. The data of
265 $0.25^{\circ}\times 0.25^{\circ}$ was downloaded for the period of 1961-2007 and converted into map form using



266 ArcGIS and exported to ERDAS Imagine. The grids for which data were downloaded and used in
267 this study include Devprayag (altitude 469m), Tehri (608m), Rudraprayag (612m), Karnprayag
268 (784m), Joshimath (1446m) and Badrinath (3136m).

269 Daily stream flow data collected from Central Water Commission (CWC) for gauging
270 station located in the study area were used for model calibration and validation purpose. The
271 discharge gauging station Devprayag-Z9 is located downstream of the confluence of Bhagirathi and
272 Alaknanda rivers at Devprayag. The data measured at Devprayag-Z9 site were used to model the
273 Ganga River Basin up to Devprayag.

274

275 **3.1 Land Use and Soil Data**

276 Land use is one of the most important factors affecting runoff, soil erosion and evapotranspiration
277 in a watershed (Neitsch et al., 2005).

278 In the Ganga basin up to Devprayag, the most dominant land use/ land cover are open forest,
279 dense forest, barren land, snow cover area and range land covering 23.28%, 20.99%, 13.41%,
280 36.4% and 5.9% of the total basin area, respectively (Figure 2). For soils, Orthents (66%),
281 typicdorthents (21%) and typiccryochrepts (12%) are the most dominant soils having 2, 3 and 3
282 layers respectively in the basin (Figure 3).

283

284 **3.2 Model Set Up**

285 In the setup of SWAT model for the study catchment, the first step is identification and delineation
286 of hydrological response units (HRUs). River network for Ganga basin up to Devprayag were
287 delineated from ASTER DEM by using the analytic technique of the ArcSWAT 2009 GIS
288 interface(Figure 4).To obtain a reasonable numbers of HRUs within each subbasin, a unique
289 combination of landuse and soil (thresholds of 10% in land use/land cover and 5% in soil type)
290 were used. In this procedure, the Ganga River Basin was divided into 7 sub-basins and 126 HRUs
291 as shown in Figure 5. These set up ensures a stream network definition that satisfactorily represents
292 the dominant land uses and soils within each subbasin and at the same time, a reasonable number of
293 HRUs are created in each sub-basin.

294 The SWAT model has a large number of parameters that describe the different hydrological
295 taking place in the study basin. During calibration process, model parameters were systematically
296 adjusted to obtain results that best match with the observed values. In the validation process, the
297 catchment response was simulated by using the parameters finally obtained during the calibration
298 process. For evaluating the model performance computed hydrographs was compared with the
299 observed hydrograph. It may be stated here that the streamflow data for the Ganga basin is
300 classified and cannot be disclosed. Hence, we have shown scaled values of the flows in various
301 graphs of Ganga basin.

302 The length of calibration data is an important factor in model calibration. The available data
303 is usually partitioned in two sets: calibration data and validation data. Usually, calibration is carried
304 out by using more years of data; say about 60 – 75 % of the available data. Typical questions that
305 arise in this respect are: how much data are necessary/enough to obtain a good model calibration



306 and what are the characteristics that the calibration data should have to maximize the chances of
307 obtaining reliable parameter estimates? Ideally, model calibration should result in parameter values
308 that produce the best overall agreement between simulated and observed values (discharge in this
309 case). Yapo et al., 1996 found that for the watersheds similar to their study area, approximately 8
310 years of data may be necessary to obtain a calibration that is relatively insensitive to the period
311 selected and that the benefits of using more than 8 years of calibration data may be marginal.
312 Regarding the characteristics, parameter identifiability significantly improves when the all the
313 hydrologic components are activated during the calibration period.

314 Statistical performance measures of the hydrological models are computed to determine
315 how the values simulated by the model match with those observed. For this study, the statistical
316 criteria that were used to evaluate model performance were the goodness-of-fit (R^2), the Nash-
317 Sutcliffe efficiency index (NSE) and coefficient of regression line multiplied by the coefficient of
318 determination (bR^2). The model performance is considered to be better as the values of R^2 and NSE
319 approach unity.

320 The observed daily stream flow data from year 1990 to 1998 were used to calibrate the
321 SWAT model and the model was validated by using the data from the year 1999 to 2005. Data for
322 the first two years (1990 and 1991) were reserved as “warm-up” period (to overcome the errors due
323 to incorrect initial conditions, the results of model run for a few initial periods are not used in
324 analysis of results. These initial periods are termed as the warm up period). Thus the model
325 calibration statistics was evaluated for the period 1992-1998.

326

327 **4 RESULTS AND DISCUSSIONS**

328 Initially, the SWAT-CUP which uses Sequential Uncertainty Fitting (SUFI2) algorithm
329 developed by Abbaspour et al., 2007 was used in this study. SUFI2 is a multi-site, semi-automated
330 global search procedure for model calibration and uncertainty analysis. The sources of uncertainties
331 which includes temperature and rainfall parameters and measured data are accounted for in SUFI2.
332 SUFI2 uses P-factor, the percentage of measured data bracketed by the 95% prediction uncertainty
333 (95PPU), and the R-factor average width of the 95PPU band divided by the standard deviation of
334 the measured data, to assess uncertainty. Abbaspour et al., 2007 have described SUFI2 algorithm in
335 detail.

336 While studying the SUFI2 calibration results, it was seen that in the table of monthly values
337 of various water balance components produced by SWAT, snowfall had fairly high values in
338 monsoon months whereas the study area does not receive snowfall in monsoon months (June to
339 September). PLAPS and TLAPS were the parameters controlling the temporal distribution of
340 precipitation (whether rain or snow). The calibrated values of PLAPS and TLAPS from the SWAT-
341 CUP were 8.5 and -5.83. To have realistic values of precipitation distribution, TLAPS and PLAPS
342 were changed systematically and TLAPS equal to -4.0 and PLAPS equal to 8.55 yielded
343 precipitation values which were realistic for the study area. However, as a result of this change,



344 there were many significant deviations between observed and simulated hydrographs. In particular,
345 the recession limbs and hydrograph during lean season had poor match as shown in Figure. 6.

346 At this stage, sensitivity analysis of model parameters was performed. Twenty calibrated
347 parameters including seven snowmelt related parameters were used for sensitivity analysis. The
348 sensitivity rank, default value, range of the parameter values and the optimal values for Devprayag
349 sites in the basin are given in Table 2. The remaining parameters were not much sensitive for the
350 model output. A number of SWAT parameters are related to snow but out of these, three parameters,
351 viz. maximum temperature index melt factor SMFMX, the snowmelt base temperature SMTMP and
352 the minimum temperature index melt factor SMFMN were found to be important.

353 The parameters were ranked in terms of their sensitivity to the model calibration. These
354 sensitive parameters were mainly responsible for changes in model output during calibration.
355 Results showed that CN is the most sensitive parameter to changes in discharge. Next to CN, the
356 other parameters that were found to be sensitive are those related to soil and groundwater. Among
357 these, ALPFA_BF is the baseflow recession constant.

358 For proper simulation of the hydrograph during post monsoon and lean season, the changes
359 in hydrograph in response to changes in several key parameters were also studied. It is noted during
360 sensitivity analysis that changes in some model parameters may cause different type of changes in
361 the simulated discharge in different seasons (monsoon and post monsoon). For instance, if the value
362 of CN is increased, the simulated streamflow increased from September to May but decreased from
363 June to August. When the value of ALPHA_BF was reduced, the simulated streamflow was found
364 to increase from October to March and decrease from April to September. When the value of
365 SOL_AWC was decreased, the simulated streamflow increased from September to February and
366 decreased from March to August. When the value of SOL_K was increased, the simulated
367 streamflow increased from February to August but decreased from September to January. When the
368 value of GW_DELAY was increased, the simulated streamflow increased from March to August
369 and decreased from September to February.

370 To improve the match between observed and simulated hydrographs in terms of recession
371 limb and base flow, it was hypothesized that the movement of water through soil and ground water
372 zone is not being properly modeled. Since baseflow was being under-simulated, more water should
373 be allowed to enter the sub-surface zone, stay there for some time, and then emerge as baseflow.
374 Accordingly, several simulations were carried out by changing the soil and ground water related
375 parameters till the simulated hydrographs shows a good match with the observed hydrograph. The
376 parameters that were systematically tuned include ALPHA_BF, SOL_AWC, SOL_K, and
377 GW_DELAY. Two statistical performance measures (coefficient of determination R^2 and NSE) and
378 visual inspection of the plot between observed and computed hydrographs were used to evaluate the
379 performance of the model in simulating streamflows and to decide which parameters to change.

380 The hydrographs of the observed and simulated daily and monthly flows for the calibration
381 period (1992-1998) for the Ganga Basin up to Devprayag are shown in Figure 7a and 9a. It is seen



382 that the overall shape of the simulated hydrograph is matching well with the observed hydrograph
383 and the recession behaviour is also well simulated now. A few of the observed high peaks have
384 been simulated well while some of the peak values do not match well. The time series of the
385 observed and simulated daily and monthly hydrographs for the validation period are shown in
386 Figure 8a and 10a. It is seen from the graph that the simulated hydrograph correlates significantly
387 well with observed hydrograph. Scatter plot between observed and simulated daily and monthly
388 discharges for the calibration data (Figure 7b and 9b) indicate even distribution of most of the
389 points around the 1:1 line. Of course, a few data points are away from the line. Further, for the
390 validation period, the scatter plot for daily and monthly (Figure 8b and 10b) also shows the points
391 of the simulated flows are close to the 45° line.

392 The statistical performance indicators for calibration and validation for the Ganga basin up
393 to Devprayag are given in Table 3. The coefficient of determination (R^2) was 0.69 and 0.95 for
394 daily and monthly calibration period and 0.57 and 0.94 for daily and monthly during validation
395 period. The NSE was computed as 0.64 and 0.80 for daily and monthly calibration period and
396 0.49 and 0.85 for daily and monthly validation period. Thus one may conclude that the indices for
397 monthly data are excellent and can be termed as very good for the daily data. Figure 11 show the
398 plot of observed and computed hydrograph for one year. It can be seen that some peaks have been
399 properly simulated but some are not. It is highlighted that the density of raingauge network in the
400 study area is grossly inadequate. Due to this many rainfall events that occur in the vicinity
401 contribute large volumes of water in the model even though their spatial coverage may be small. On
402 the other hand, if the event does not occur around the raingauge will be missed even though it may
403 have a large spatial coverage.

404 For calibration and validation, various water balance components are given in Table 4. The
405 water balance components include: the total amount of precipitation, actual evapotranspiration,
406 snowmelt runoff, and water yield. Here, water yield includes surface runoff, lateral flow to stream
407 and water from shallow aquifer that returns to river reach. The results indicate that contribution
408 from direct surface runoff is small in the water yield and the main contribution to water yield is
409 through lateral flow and ground water flow. ET comes out to be 43-46% of precipitation. As
410 catchment of Ganga river up to Devprayag site has comparatively less snow covered area, ET is at
411 higher rate. The snowmelt runoff contribution at Devprayag site comes out to be 20% and 13% of
412 the water yield during calibration and validation respectively. The water yield, i.e. sum of surface
413 runoff, lateral runoff and ground water contribution in stream flow comes out be about 57-58% of
414 the precipitation. In the basin, interflow contributes significantly to the water yield as compared to
415 shallow groundwater.

416

417 5 CONCLUSIONS

418 This study has attempted to simulate the response of hilly parts of a Himalayan river basin, viz., the
419 Ganga basin up to Devprayag. The values of R^2 and NSE for calibration (1992-1998) and validation
420 (1999-2005) vary between 0.69 and 0.64 and can be considered as good (as per Moriasi et al., 2007)



421 for the basin given the availability of meteorological and pedological data. Overall, the hydrograph
 422 shape could be reproduced satisfactorily although all the peaks and the recession limbs could not be
 423 reproduced very well. Thus, the SWAT model can be considered to be a good tool to model the
 424 discharge hydrograph and various water balance components for a Himalayan basin.

425 Water yield for the basin is ranging between 57-58% of the precipitation. Snow/glacier melt
 426 contribution is 13-20% for the Ganga basin. In the Ganga basin, interflow contributes significantly
 427 to the water yield. However, these results are required to be buttressed by more detailed hydrologic
 428 modeling of some more river basins to investigate their response mechanism. To that end, more
 429 attention is needed to strengthen spatial, soil and hydrometeorological database including snowfall
 430 for the study basins by installing automatic weather stations to measure precipitation (rain and
 431 snow) and other climatic variables at various elevations. Isotope analysis may be carried out to
 432 separate the runoff components and compare the results with hydrologic model.

433

434 REFERENCES

- 435 Abbaspour, K. C., Yang, j., Maximov, I., Siber, R., Bogner, K., Mieleitner, J., Zobrist, J., and
 436 Srinivasan, R.: Modelling hydrology and water quality in the pre-alpine/alpine Thur watershed
 437 using SWAT. *Journal of Hydrology*, 333, 413– 430, 2007.
- 438 Anderson, E.A.: A Point Energy and Mass Balance Model of Snow Cover. In: Development of a
 439 Snowfall-Snowmelt Routine for Mountainous Terrain for the Soil Water Assessment Tool
 440 (SWAT), T.A., Fontaine, T.S. Cruickshank, J.G. Arnold, and R.H. Hotchkiss (Editors), 1976.
- 441 Arnold, J.G., Srinivasan, R., Muttiah, R.S., and Williams, J.R.: Large area hydrologic modeling and
 442 assessment part I: model development *J. Am. Water Resour. Assoc.*, 34, pp. 73–89, 1998.
- 443 Awan, U.K., Liaqat, U.W., Choi, M., and Ismaeel, A.: A SWAT modeling approach to assess the
 444 impact of climate change on consumptive water use in Lower Chenab Canal area of Indus
 445 basin. *Hydrology Research*, in press, 2016.
- 446 Bergstrom, S.: The HBV model-its structure and applications. SMHI Reports RH, No. 4,
 447 Norrkpoing, Sweden, 1992.
- 448 Fontaine, T.A., Cruickshank, T.S., Arnold, J.G., and Hotchkiss, R.H.: Development of a snowfall-
 449 snowmelt routine for mountainous terrain for the soil water assessment tool (SWAT). *J Hydrol*,
 450 262(1–4):209–223, 2002.
- 451 Yasin, H.Q. and S.Clemente, R.: Application of SWAT Model for Hydrologic and Water Quality
 452 Modeling in Thachin River Basin, Thailand, *Arabian Journal for Science and Engineering*,
 453 Volume 39, Issue 3 , pp 1671-1684, 2012.
- 454 Hartman, M.D., Baron, J.S., Richard, B.L., Donald, W.C., Larry, E.B., Glen, E.L., and Christina,
 455 T.: Simulations of Snow Distribution and Hydrology in a Mountain Basin. *Water Resources*
 456 *Research*, 35(5):1587-1603, 1999.
- 457 Hock, R.: Temperature index melt modelling in mountain areas. *J Hydrol* 282(1–4):104–115.
 458 doi:10.1016/s0022-1694(03)00257-9, 2003.
- 459 Immerzeel, W. W., Pellicciotti, F. and Bierkens, M. F. P.: 1004 Rising river flows throughout the
 460 twenty-first century in two Himalayan glacierized watersheds, *Nature Geosci*,
 461 doi:10.1038/ngeo1896, 2013.
- 462 Jain, S.K., Tyagi, J., and Singh V.: Simulation of runoff and sediment yield for a Himalayan
 463 Watershed using SWAT model. *J. Water Resource and Protection*, 2, 267-281, 2010.



- 464 Jha, M. K.; Arnold, J. G., and Gassman, P. W.: "Water Quality Modeling for the Raccoon River
465 Watershed Using SWAT". CARD Working Papers. Paper 452.
466 http://lib.dr.iastate.edu/card_workingpapers/452, 2006.
- 467 Khan, A.D., Ghoraba, S., Arnold, J.G., and Di Luzio, M.: Hydrological modeling of upper Indus
468 Basin and assessment of deltaic ecology. *International Journal of Modern Engineering*
469 *Research*. 4(1):73-85, 2014.
- 470 Kushwaha, A., and Jain, M.K.: Hydrological simulation in a forest dominated watershed in
471 Himalayan region using SWAT model *Water Resour. Manag.*, 27, pp. 3005–3023.
472 <http://dx.doi.org/10.1007/s11269-013-0329-9>, 2013.
- 473 Lemonds, P.J., and McCray, J.E.: Modeling hydrology in a small rocky mountain watershed serving
474 large urban populations. *J. American Water Resour. Assoc.* 43(4): 875-887, 2007.
- 475 Li, H., Beldring, S., Xu, C.Y., Huss, M., and Melvold, K.: Integrating a glacier retreat model into a
476 hydrological model -- case studies on three glacierised catchments in Norway and Himalayan
477 region. *Journal of Hydrology* 527, 656-667. doi:10.1016/j.jhydrol.2015.05.017, 2015.
- 478 Li, H., Xu, C.Y., Beldring, S., Tallaksen, T.M., and Jain, S.K.: Water Resources under Climate
479 Change in Himalayan basins. *Water Resources Management*, in press. DOI:10.1007/s11269-
480 015-1194-5, 2016.
- 481 Li, L., Engelhard, M., Xu, C.Y., Jain, S.K., and Singh, V.P.: Comparison of satellite based and
482 reanalysed precipitation as input to glacio hydrological modeling for Beas river basin, Northern
483 India. *Cold and Mountain Region Hydrological Systems under Climate Change: Towards*
484 *Improved Projections*. IAHS Publ. 360. 45-52, 2013.
- 485 Liston, G.E., and Elder, K.: A distributed snow evolution modeling system (SnowModel). *Journal*
486 *of Hydrometeorology*, 7: 1259–1276, 2006.
- 487 Luo, Y., Arnold, J., Liu, S., Wang, X., and Chen, X.: Inclusion of glacier 1050 processes for
488 distributed hydrological modeling at basin scale with application to a watershed in Tianshan
489 Mountains, northwest China, *J. Hydrol.*, 477, 72-85, 2013.
- 490 Moriasi, D.N., Arnold, J.G., Van Liew, M.W., Bingner, R.L., Harmel, R.D., and Veith, T.L. :
491 Model evaluation guidelines for systematic quantification of accuracy in watershed
492 simulations. *Transactions of the American Society of Agricultural and Biological Engineers*,
493 50(3): 885–900, 2007.
- 494 Neitsch, S.L., Arnold, J.G., Kiniry, J.R., and Williams, J.R.: Soil and water assessment tool
495 (SWAT) theoretical documentation. Blackland Research Center, Texas Agricultural
496 Experiment Station, Temple, TX, p 781, 2001.
- 497 Neitsch, S.L., Arnold, J.G., Kiniry, J.R., Srinivasan, R., and Williams, J.R.: Soil and Water
498 Assessment Tool, User Manual, Version 2000. Temple, Tex.: Grassland, Soil and Water
499 Research Laboratory, 2002.
- 500 Neitsch, S.L., Arnold, J.C., Kiniry, J.R., Williams, J.R., and King, K.W.: Soil and Water
501 Assessment Tool Theoretical Documentation. Version 2000. Texas Water Resources Institute,
502 College Station, Texas, USA, 2002a.
- 503 Neitsch, S.L., Arnold, J.C., Kiniry, J.R., Williams, J.R., and King, K.W.: Soil and Water
504 Assessment Tool User's Manual. Version 2000. Texas Water Resources Institute, College
505 Station, Texas, USA, 2002b.
- 506 Neitsch, S.L., Arnold, J.G., Kiniry, J., and Williams, J.R.: Soil and water assessment tool theoretical
507 documentation, USDA Agricultural Research Service and. Texas A&M Blackland Research
508 Center, Temple, 2005.



- 509 Pandey, A., Daniel, L., and Jain, S.K.: Assessment of hydropower potential using spatial
510 technology and SWAT modeling in the Mat river of Southern Mizoram, India. *Hydrological*
511 *Sciences Journal* (in press), 2014.
- 512 Pradhanang, S.M., Anandhi, A., Rajith, M., Zion, M.S., Pierson, D.C., Schneiderman, E.M.,
513 Matonse, A., and Frei, A.: Application of SWAT model to assess snowpack development and
514 streamflow in the Cannonsville watershed, New York, USA. *Hydrol. Process.* **25**, 3268–3277,
515 2011.
- 516 Qiu, Z. and Wang, L.: "Hydrological and Water Quality Assessment in a Suburban Watershed with
517 Mixed Land Uses Using the SWAT Model." *J. Hydrol. Eng.*, 10.1061/(ASCE)HE.1943-
518 5584.0000858, 816-827, 2014.
- 519 Shawul, A. A., Alamirew, T., and Dinka, M. O.: Calibration and validation of SWAT model and
520 estimation of water balance components of Shaya mountainous watershed, Southeastern
521 Ethiopia, *Hydrol. Earth Syst. Sci. Discuss.*, 10, 13955-13978, doi:10.5194/hessd-10-13955-
522 2013, 2013.
- 523 Shrestha, B., Babel, M.S., Maskey, S., van Griensven, A., Uhlenbrook, S., Green, A. and
524 Akkharath, I.: Impact of 495 climate change on sediment yield in the Mekong River
525 Catchment: a case study of the Nam Ou Catchment, Lao 496 PD, *Hydrol. and Earth Syst. Sci.*,
526 17(1), 1-20, 2013.
- 527 Singh, H.V., Kalin, L., Morrison, A., Srivastava, P., Lockaby, G., and Pan, S.: Post-validation of
528 SWAT model in a coastal watershed for predicting land use/cover change impacts. *Hydrology*
529 *Research*, DOI: 10.2166/nh.2015.222, in press, 2016.
- 530 Spruill, C.A., Workman, S.R., Taraba, J.L.: Simulation of daily and monthly stream discharge from
531 small watersheds using the SWAT model. *Trans. ASAE* 43(6): 1431-1439, 2000.
- 532 Stehr, A., Debels, P., Arumi, J.L., Romero, F., and Alcayaga, H.: Combining the Soil and Water
533 Assessment Tool (SWAT) and MODIS imagery to estimate monthly flows in a data scarce
534 Chilean Andean basin. *Hydrological Sciences Journal* 54: 1053–1067, 2009.
- 535 Tamm, O., Luhamaa, A., and Tamm, T.: Modelling future changes in the North-Estonian
536 hydropower production by using SWAT. *Hydrology Research*, in press, 2016.
- 537 Troin, M., and Daniel, C.: Evaluating the SWAT's snow hydrology over a Northern Quebec
538 watershed. *Hydrological Processes*, 28(4), 1858–1873, 2014.
- 539 Tyagi, J. V., Rai, S. P., Qazi, N., and Singh, M. P.: Assessment of discharge and sediment transport
540 from different forest cover types in lower Himalaya using Soil and Water Assessment Tool
541 (SWAT). *International Journal of Water Resources and Environmental Engineering*, 6(1), 49-
542 66, 2014.
- 543 Yapo, P. O., Gupta, H. V., and Sorooshian, S.: Automatic calibration of conceptual rainfall-runoff
544 models: Sensitivity to calibration data. *Journal of Hydrology*, 181(1-4), 23-48, 1996.
- 545 Zhang, X.S., Srinivasan, R., Debele, B., and Hao, F.H.: Runoff simulation of the headwaters of the
546 Yellow River using the SWAT model with three snowmelt algorithms. *J Am Water Resource*
547 *Assoc.*, 44(1):48–61. doi:10.1111/j.1752-1688.2007.00137, 2008.
- 548 Zhao, R. J., Liu, X. R., and Singh, V. P.: The Xinanjiang model. *Computer models of watershed*
549 *hydrology*, 215–232. Water Resources Publications, Highlands ranch, Colorado, 1995.
- 550
551
552
553
554
555



556

557

558 Table 1: Sources and description of the input data for the Ganga Basin up to Devprayag

559

Data Type	Source	Spatial/ Temporal Resolution	Description
Topography	http://gdem.ersdac.jspacesystems.or.jp	90 m	Aster Digital Elevation Model
Land use/Land cover	www.iitd.ac.in	90 m	Land-use Classification
Soils	www.iitd.ac.in	90 m	Soil Classification
Weather Data	APHRODITE DATA	1.0 deg 0.25 deg	Temperature, Solar Radiation, Wind Speed, Precipitation, Data
Stream Flow	Central Water Commission, Dehradun	Daily	Daily stream flows measured at the gauging stations

560

561

562 Table 2: Description of 20 calibration parameters: Sensitivity rank, Default value, Range and
 563 Optimal value

Parameters	Description	Sensitivity Rank	Default value	Range	Optimal value
CN2	Initial SCS runoff curve number for moisture condition II	1	77-92	35-98	55-92
TLAPS	Temperature Lapse Rate	2	0	-10 to 10	-4.0
SOL_AWC	Available water capacity of the soil layer (mm/mm)	3	0.067 – 0.146	0 - 1	0.024 – 0.053
SOL_K	Saturated hydraulic conductivity of soil (mm/hr)	4	1.95 – 121.12	0 - 2000	3.0 – 186.61



SOL_Z	Soil depth (mm)	5	60 - 170	0 -3500	30 - 300
ALPHA_BF	Base flow alpha factor (days)	6	0.084	0-1	0.07
GW_DELAY	Groundwater delay (days)	7	31	0-500	35
REVAPMN	Threshold depth of water in the shallow aquifer for "revap" to occur (mm)	8	1	0-500	499
RCHRG_DP	Deep aquifer percolation fraction	9	0.05	0-1	0.015
GW_REVAP	Groundwater revap coefficient	10	0.02	0.02 - 0.20	0.162
CH_K2	Effective hydraulic conductivity in main channel alluvium (mm/h)	11	0	-0.01 - 500	20.43
ESCO	Soil evaporation compensation factor	12	0.95	0-1	0.40
PLAPS	Precipitation Lapse Rate	13	0	-1000 to 1000	8.55
SMTMP	Snowmelt base Temperature (°C)	14	0.5	-5 to 5	-3.05
SMFMN	Minimum melt rate for snow during year (mm H ₂ O/°C -day)	15	4.5	0 - 10	0.80
SMFMX	Maximum melt rate for snow during year (mm H ₂ O/°C -day)	16	4.5	0 - 10	4.79
SNO50COV	Snow water content corresponding to 50% snow cover	17	0.50	0 - 1	0.48
SFTMP	Snowfall Temperature (°C)	18	1	-5 to 5	-2.79
TIMP	Snow pack temperature lag factor	19	1	0-1	0.394
SNOCOVMX	Minimum snow water content corresponding to 100% snow cover, SNO100 (SNOCOVMX- mm H ₂ O)	20	1	0 - 500	242.40



567

568

569 Table 3: Statistical performance indicators for calibration and validation for Ganga River Basin up
570 to Devprayag

571

Daily/Monthly	Calibration (1992-1998), Validation(1999-2005)	R ²	NSE
	Calibration	0.69	0.64
Daily	Validation	0.57	0.49
	Calibration	0.95	0.80
Monthly	Validation	0.94	0.85

572

573

574

575

576 Table 4: Water balance components in mm

	Precipitation	ET	Surface Runoff	Lateral flow	Ground water flow	Water yield	Snow fall	Snow melt
Calibration	1236.1	484.8	96.63	297.30	293.92	686.87	140.74	73.84
Validation	1203.3	512.1	74.24	299.37	290.05	662.81	110.57	48.87

577

578

579

580

581

582

583

584

585

586

587

588

589

590

591

592

593

594

595

596



597
598
599
600
601
602
603
604
605
606
607
608
609
610
611
612
613
614
615
616
617
618
619
620
621
622
623
624
625
626
627
628
629
630
631
632
633
634
635
636
637
638
639
640
641
642
643

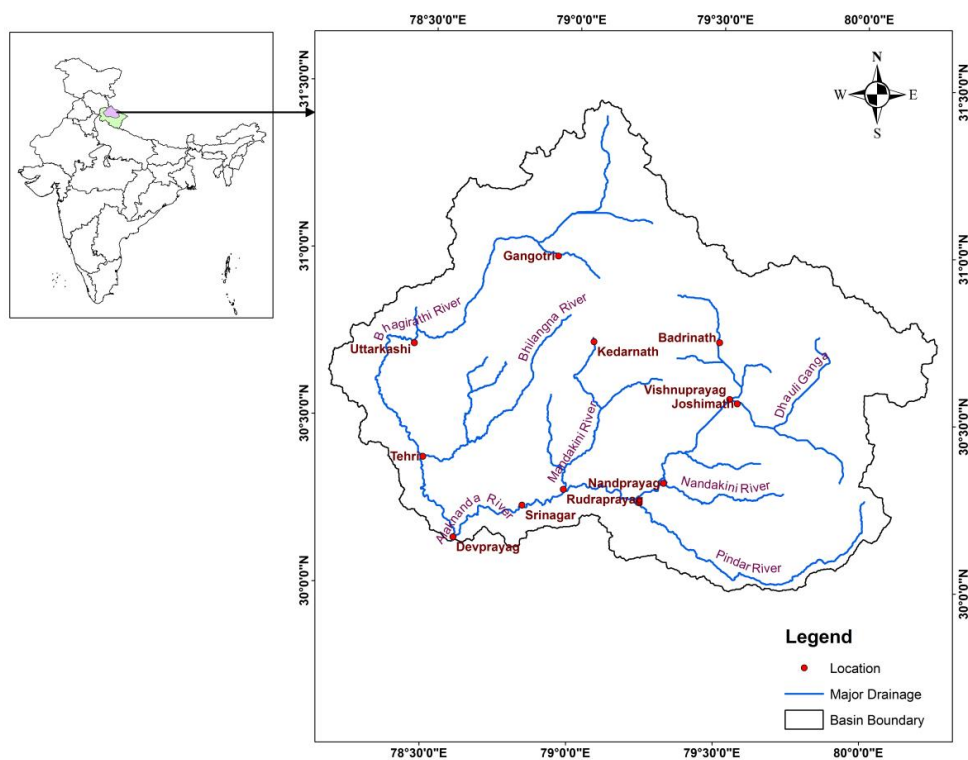


Figure 1: Index map of Ganga basin up to Devprayag



644
645
646
647
648
649
650
651
652
653
654
655
656
657
658
659
660
661
662
663
664
665
666
667
668
669
670
671
672
673
674
675
676
677
678
679
680
681
682
683
684
685
686
687
688
689
690

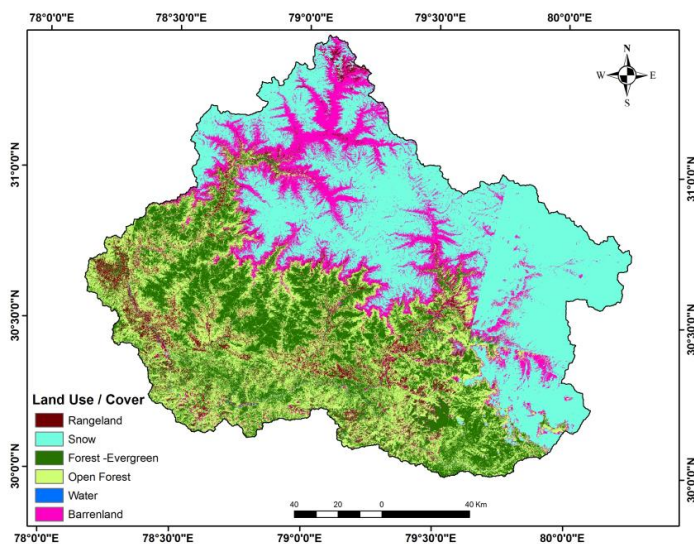


Figure 2: Land use/cover of Ganga basin up to Devprayag

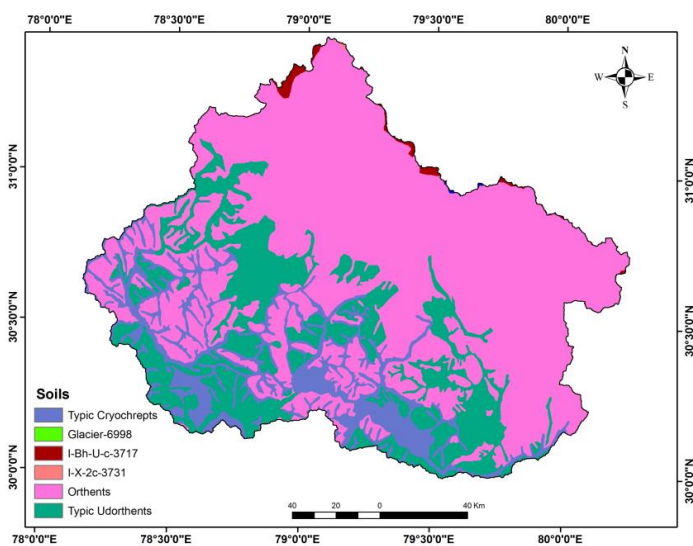


Figure 3: Soil map of Ganga basin up to Devprayag



691
692
693
694
695
696
697
698
699
700
701
702
703
704
705
706
707
708
709
710
711
712
713
714
715
716
717
718
719
720
721
722
723
724
725
726
727
728
729
730
731
732
733
734
735

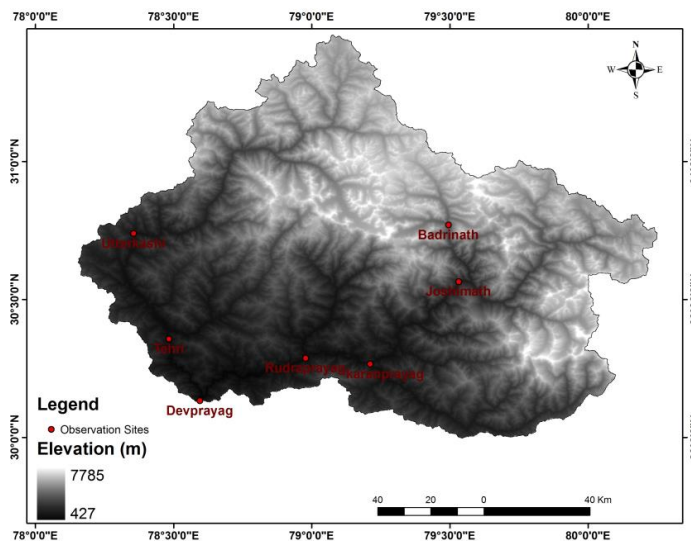


Figure 4: DEM of Ganga basin up to Devprayag

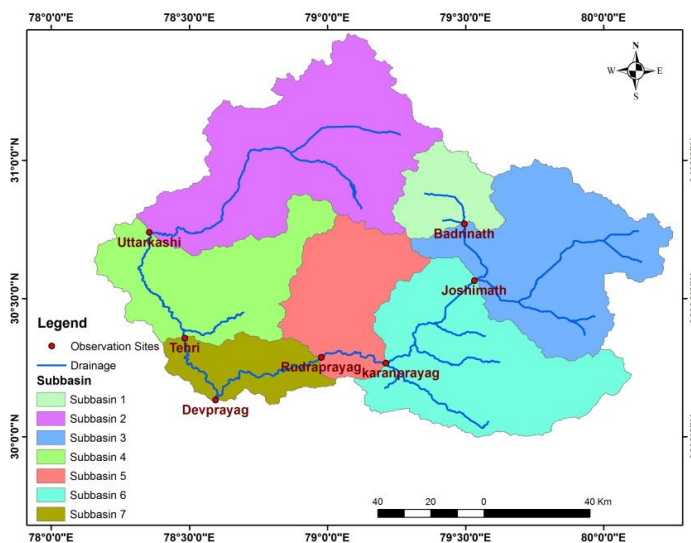


Figure 5: Sub basin map of Ganga basin up to Devprayag



736
737
738
739
740
741
742
743
744
745
746
747
748
749
750
751
752
753
754
755
756
757
758
759
760
761
762
763
764
765
766
767
768
769
770
771
772
773
774
775
776
777
778
779
780
781
782

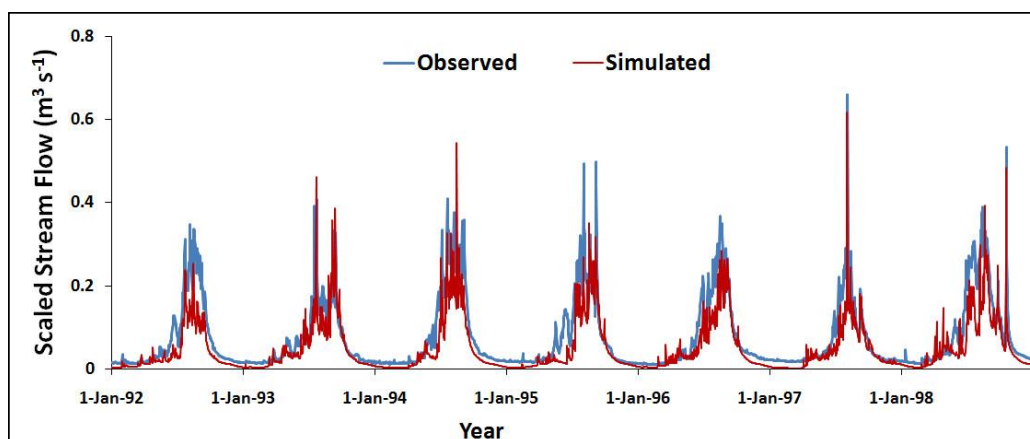


Figure 6: Comparison of daily observed and simulated stream flow hydrograph of Ganga basin up to Devprayag during calibration period (1992-1998) during iteration process



783
784
785
786
787
788
789
790
791
792
793
794
795
796
797
798
799
800
801
802
803
804
805
806
807
808
809
810
811
812
813
814
815
816
817
818
819
820
821
822
823
824
825
826
827
828
829

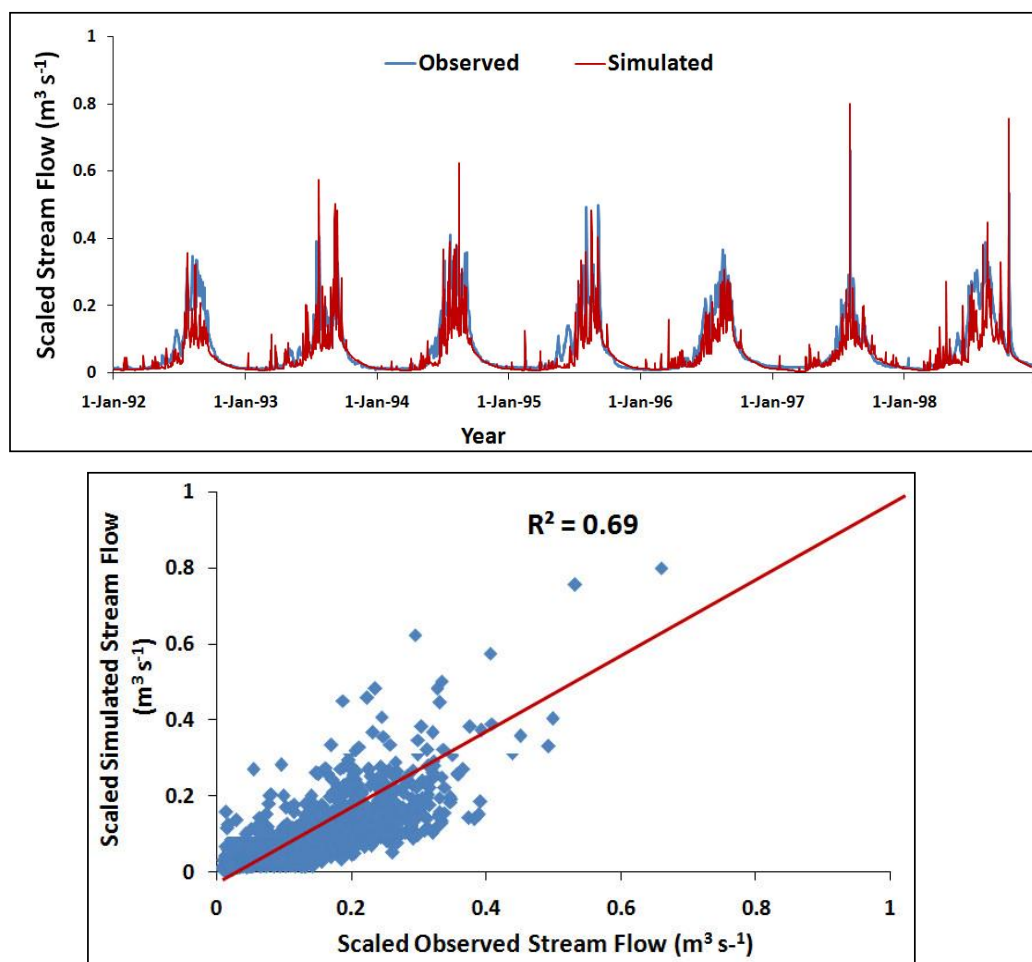


Figure 7: Comparison of a) daily observed and simulated stream flow hydrograph of Ganga basin up to Devprayag during calibration period (1992-1998), and b) scatter plot



830
831
832
833
834
835
836
837
838
839
840
841
842
843
844
845
846
847
848
849
850
851
852
853
854
855
856
857
858
859
860
861
862
863
864
865
866
867
868
869
870
871
872
873
874
875
876

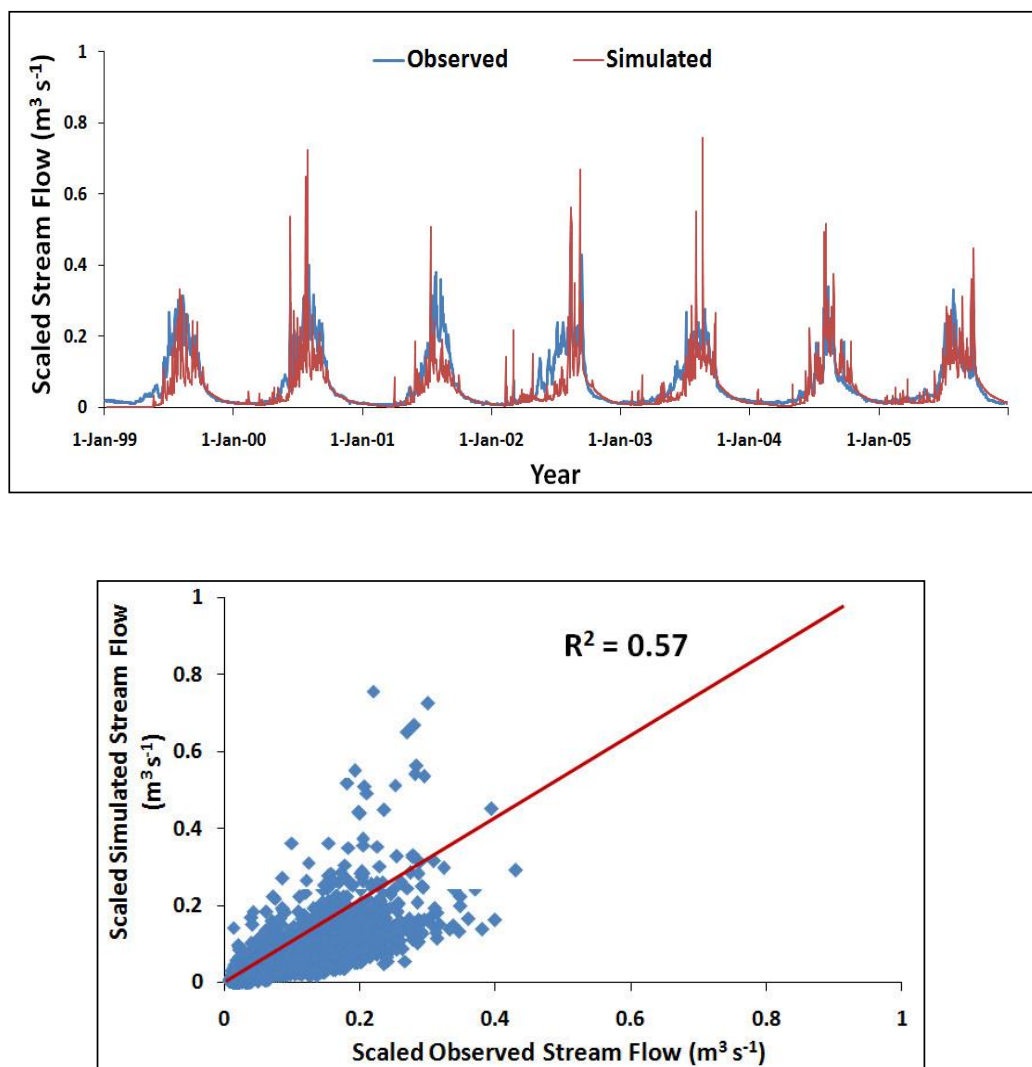


Figure 8: Comparison of a) daily observed and simulated stream flow hydrograph of Ganga basin up to Devprayag during validation period (1999-2005), and b) scatter plot



877
878
879
880
881
882
883
884
885
886
887
888
889
890
891
892
893
894
895
896
897
898
899
900
901
902
903
904
905
906
907
908
909
910
911
912
913
914
915
916
917
918
919
920
921
922
923

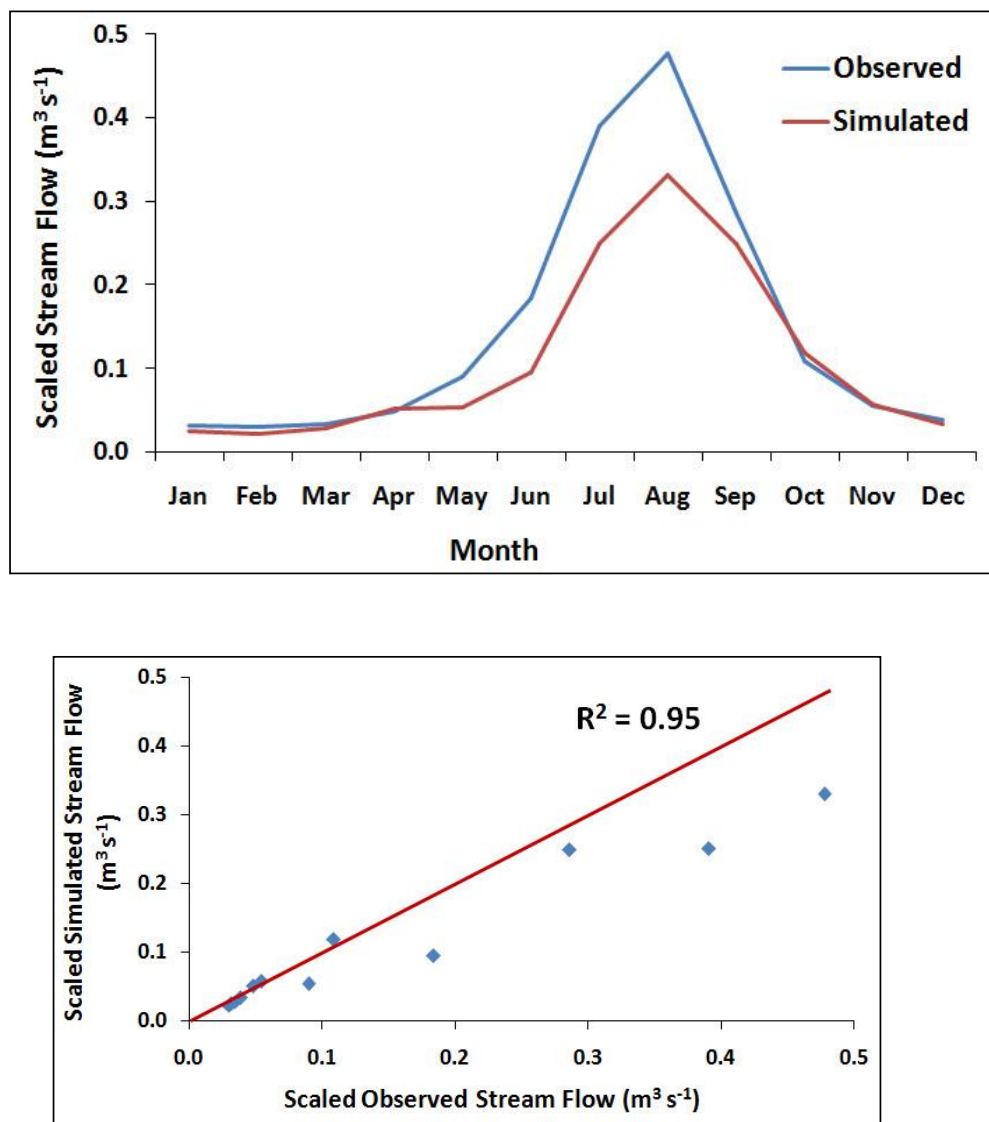


Figure 9: Comparison of a) Monthly observed and simulated stream flow hydrograph of Ganga basin up to Devprayag during calibration period (1992-1998), and b) scatter plot



924
925
926
927
928
929
930
931
932
933
934
935
936
937
938
939
940
941
942
943
944
945
946
947
948
949
950
951
952
953
954
955
956
957
958
959
960
961
962
963
964
965
966
967
968
969
970

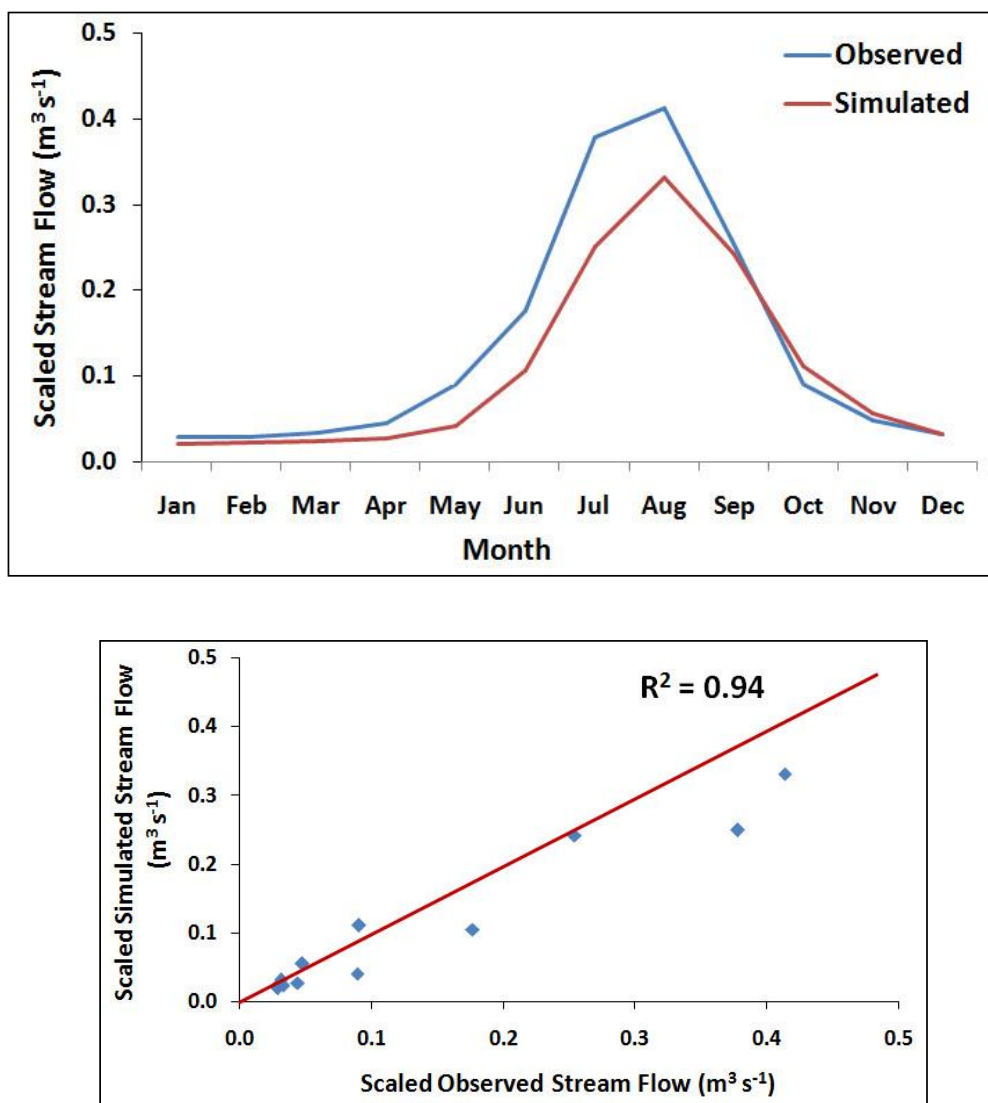


Figure 10: Comparison of a) Monthly observed and simulated stream flow hydrograph of Ganga basin up to Devprayag during Validation period (1999-2005), and b) scatter plot.



971
972
973
974
975
976
977
978
979
980
981
982
983
984
985
986
987
988
989

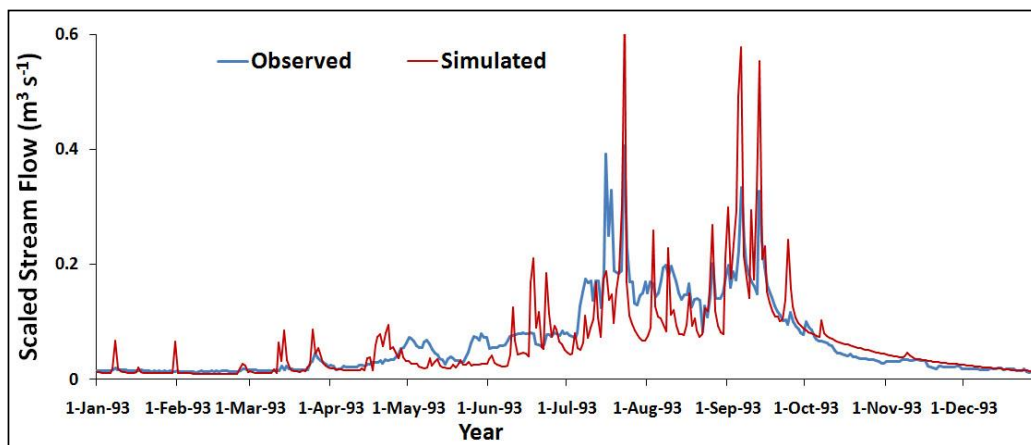


Figure 11: Daily observed and simulated stream flow hydrograph of Ganga basin up to Devprayag for the year 1993.